INSTITUTES FOR ENVIRONMENTAL RESEARCH
National Severe Storms Laboratory
Norman, Oklahoma
July 1967

Note on Probing Balloon Motion by Doppler Radar

ROGER M. LHERMITTE

Technical Memorandum IERTM-NSSL 34

U.S. DEPARTMENT OF COMMERCE / ENVIRONMENTAL SCIENCE SERVICES ADMINISTRATION

U.S. DEPARTMENT OF COMMERCE
ENVIRONMENTAL SCIENCE SERVICES ADMINISTRATION
INSTITUTES FOR ENVIRONMENTAL RESEARCH

Institutes for Environmental Research Technical Memorandum -NSSL 34

NOTE ON PROBING BALLOON MOTION BY DOPPLER RADAR

Roger M. Lhermitte

NATIONAL SEVERE STORMS LABORATORY
TECHNICAL MEMORANDUM NO. 34

NORMAN, OKLAHOMA
JULY 1967

ENVIRONMENTAL SCIENCE SERVICES ADMINISTRATION

INSTITUTES FOR ENVIRONMENTAL RESEARCH

NATIONAL SEVERE STORMS LABORATORY TECHNICAL MEMORANDA

The National Severe Storms Laboratory, Norman, Oklahoma, in cooperation with other government groups, and with units of commerce and education, seeks to increase understanding of severe local storms, to improve methods for detecting these storms and for measuring associated meteorological parameters, and to promote the development and applications of weather radar.

Reports by the cooperating groups are printed as NSSL Technical Memoranda, a sub-series of the ESSA Technical Memorandum series, to facilitate prompt communication of information to vitally interested parties and to elicit their constructive comments. These Memoranda are not formal scientific publications.

The NSSL Technical Memoranda, beginning with No. 28, continue the sequence established by the U.S. Weather Bureau National Severe Storms Project, Kansas City, Missouri. Numbers 1-22 were designated NSSP Reports. Numbers 23-27 were NSSL Reports, and 24-27 appeared as a subseries of Weather Bureau Technical Notes.

Reports in this series are available from the Clearinghouse for Federal Scientific and Technical Information, U.S.Department of Commerce, Sills Bldg., Port Royal Road, Springfield, Virginia 22151.

TABLE OF CONTENTS

LIST OF FIGURES

NOTE ON PROBING BALLOON MOTION BY DOPPLER RADAR[1,2]

Roger M. Lhermitte
National Severe Storms Laboratory[3]

ABSTRACT

The motion of free balloons has been analyzed with Doppler radar techniques. Balloons in the subcritical Reynolds regime exhibit periodic variations of radial velocity. These variations are explained in terms of an helicoidal balloon motion with orbit radius approximately equal to the balloon diameter and vertical wavelength 10 to 15 times larger. Large irregular oscillations of balloon motion characterize flights with Reynolds number larger than 2×10^5.

1. INTRODUCTION AND METHOD

Free balloons, which can be tracked by optical methods or by radar, have been considered as acceptable tracers for air motion and are conventionally used for wind measurement. Analysis of the small-scale variability of the wind by use of very accurate automatic tracking radars have shown, however, that the wind measurements have a typical variability related to an erratic motion of the balloons.

Small-scale irregularities of the balloon motion can be conveniently analyzed with Doppler radar, which detects variations of target range smaller than the radar wavelength. The Doppler-observed speed is the radial speed associated with the change of the balloon range as a function of time.

This paper reports investigations of small-scale motions of balloons over a range of spherical balloon sizes (12" to 72") and ascent rates (0 to 6.5 m sec^{-1}). Expandable neoprene balloons were used in experiments, but the data analysis was limited to altitudes where expansion of the balloon diameter was negligible.

---

[1] In preliminary form, this paper was presented at the Conference of the American Meteorological Society on Physical Processes in the Lower Atmosphere, March 20-22, 1967, Ann Arbor, Michigan.

[2] The program of Doppler weather radar studies at the National Severe Storms Laboratory has received substantial support from the Federal Aviation Agency.

[3] Present affiliation: Institute for Telecommunication Sciences and Aeronomy, ESSA, Boulder, Colorado.

A balloon's erratic motion seems to be controlled by a self-induced turbulence originated by its vertical speed with respect to the surrounding air [Scoggins, 1964]. Scoggins noticed that if the balloon surface in contact with the air is roughened, the amplitude of the erratic displacement of the balloon decreases and the oscillation of balloon motion becomes more regular.

The flight trajectory characteristics for expandable neoprene balloons used in our experiments have also been analyzed by MacCready [1965]. In his work the average balloon speed was computed for time intervals of 4 seconds from the position data provided by an automatic tracking FPS-16 radar.

To separate the contribution to the Reynolds number from balloon size or balloon vertical velocity, we inflated the balloons with a mixture of air and helium designed to control the lifting force with relative independence from the balloon diameter. Such a method allows choice of a large range of vertical speeds for the same balloon size.

The Doppler radar method requires that the balloon be made a good isotropic target, i.e., a perfect sphere with a uniform reflective coating. When the balloon surface reflectivity is not uniform, balloon spinning and tumbling causes a smearing of the Doppler spectrum. In practice, the balloon's inner wall was coated with "chaff" dipoles by placing a few drops of oil with chaff in the balloon, and agitating the inflated balloon. This method provides a uniform distribution of the chaff dipoles on the balloon wall and a Doppler smearing typically smaller than 0.5 m sec $^{-1}$.

The radial velocity information is obtained by processing the Doppler signal through a frequency analyzing filter bank. The spacing between filters corresponds to a velocity interval of 0.2 m sec $^{-1}$. [Lhermitte and Kessler, 1964]

Similar experiments have been done by McVehill et al, [1965]. The experiments described in this report, however, cover a larger range of balloon size and vertical ascent rate and are aimed to define a flight parameter which effectively controls the balloon self-induced turbulence.

2. THE BALLOON SELF-INDUCED TURBULENCE

Figures 1a and 1b clearly show that the balloon's variable motion is caused by the balloon's spherical shape and ascent rate.

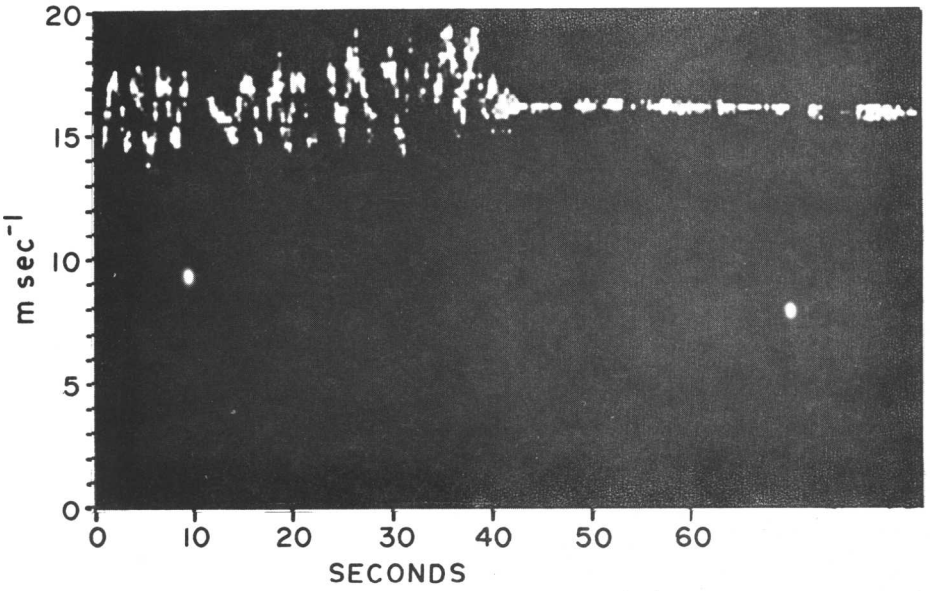

a. Oct. 3, 1966. Burst Altitude: 2,000 m. 30 gm Balloon, starting Diameter: D=32" $\theta=17.5^{o}$, $\bar{w}=4.25 m.sec^{-1}$, $R_d=1.7X10^5$.

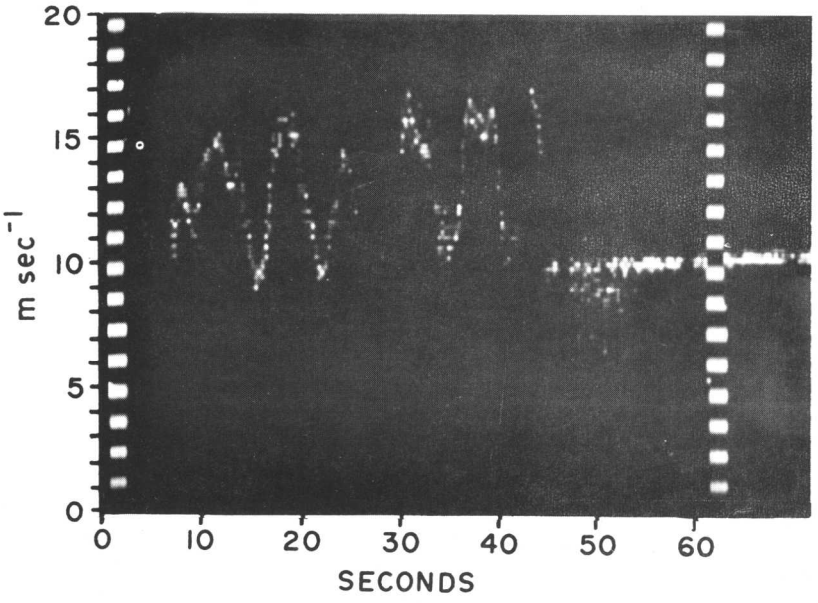

b. Oct. 11, 1966. Burst Altitude: 2,020 m. 100-gm Balloon, starting Diameter: D=48" $\theta=31.0^{o}$, $w=5.0 m.sec^{-1}$, $R_d=3.05X10^5$.

Figure 1. - Effect on balloon motion caused by balloon burst. Note that the velocity oscillations disappear completely after balloon burst at time 43/45 seconds.

In these two separate cases the radial velocity of the balloon is presented in the vicinity of the balloon burst. The characteristic variability of the balloon radial motion completely disappears after the balloon burst point. The difference between the mean motion before burst and the steady motion after burst is the contribution from the target's vertical ascent rate to the Doppler-measured radial component of velocity. The vertical velocity changes from 4 or 5 m sec^{-1} upward before burst to an estimated 2 m sec^{-1} downward after burst. Steadiness of the target motion after burst proves that the balloons moved in horizontal laminar flow and that the erratic component of the motion arose from a self-induced turbulence generated by the vertical motion relative to the air.

The small-scale variability of the balloon motion is controlled by a self-induced turbulence; this is also apparent in figure 2, which shows data acquired when the balloon was traced inside a cloud of ice crystals. Since the motion of the ice crystals was observed at the balloon location, such observations offer a basis for comparing steadiness of air motion and of balloon motion. The short-term time variations of the motion of ice crystals are small (less than 0.5 to 1 m sec^{-1}) and indicative of steady air flow. The balloon Doppler speed presents however, a large variability with peak-to-peak radial speed deviations reaching 5 to 6 m sec^{-1}. The difference of approximately 3 m sec^{-1} between the balloon's mean Doppler speed and the ice crystals' Doppler speed arises from the difference between their vertical motions and can be explained by a downward motion of ice crystals of 0.65 m sec^{-1} and an upward balloon motion of 4.3 m sec^{-1}.

3. BALLOON MOTION VARIABILITY AND ITS RELATIONSHIP TO BALLOON SIZE AND ASCENT RATE

Figure 3 shows an example of the results obtained by Doppler tracking of a small balloon. Notice that the balloon radial velocity shows peak-to-peak time variations of 1.8 m sec^{-1} with a period of 7.8 seconds. Note also the narrow Doppler spectrum, which is indicative of a good isotropic target. This type of speed variability is frequently observed for Reynolds number R_d smaller than 1×10^5. According to experiments in wind tunnels, this characterizes a subcritical flow regime around the balloon. The Reynolds number is computed from:

$$R_d = VD/\nu \quad , \qquad (1)$$

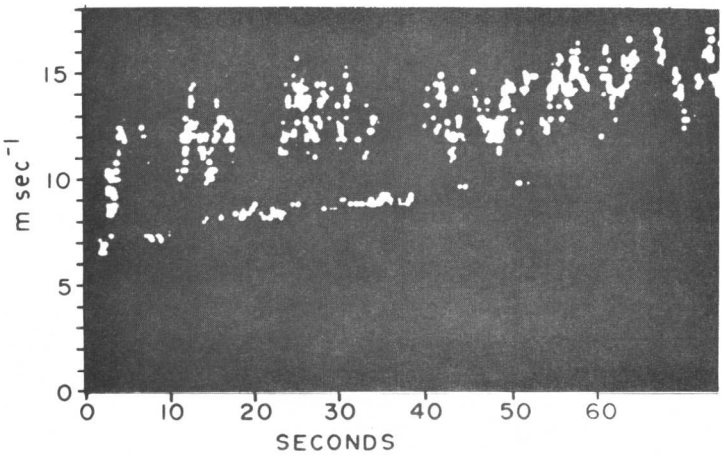

Figure 2. - Time variations of velocity compared to the motion of surrounding ice crystals. The lower trace indicates steady ice crystal motion and the balloon's erratic motion is shown in the trace above.

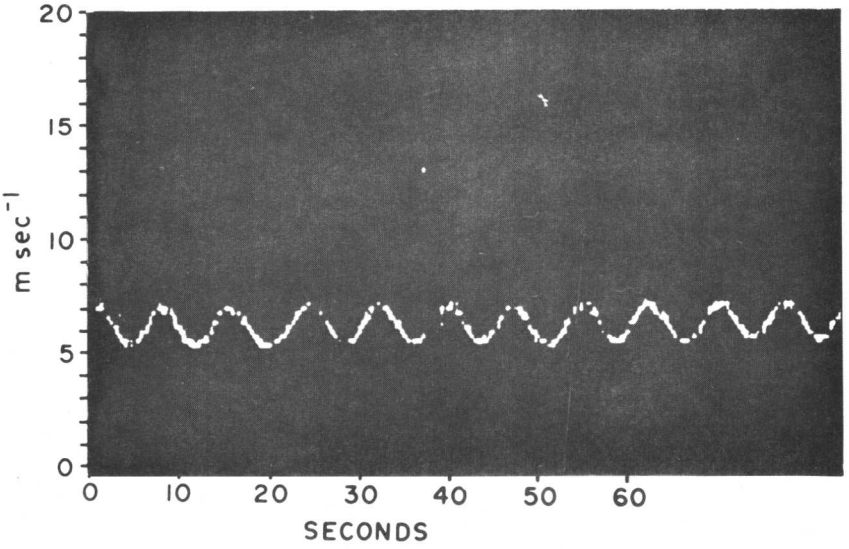

Figure 3. - Time variation of the radial speed of small balloon (D=12"). Note the sinusoidal shape indicative of the helicoidal trajectory shown in Figure 4.

where V is the motion with respect to the air, D the balloon diameter, and ν the kinematic viscosity of the air. Such sinusoidal variations of the balloon radial velocity would occur if the balloon's trajectory were helicoidal as shown in figure 4.

The trajectory parameters such as the "orbital" radius, r, and the vertical displacement for a complete revolution in the horizontal plane (vertical wavelength λ) can be computed from the Doppler data and the balloon ascent rate in the following manner. Assume a circular motion in the horizontal plane; this implies a peak-to-peak variation of the speed, V_H, that is twice the tangential speed. We know the period of revolution from the period of Doppler oscillations, T, and

$$V_H = \frac{4\pi r}{T} , \qquad (2a)$$

and the radius, r, is then

$$r = \frac{TV_H}{4\pi} . \qquad (2b)$$

As noted above, this type of balloon oscillation is typically observed with a Reynolds number about 1 X 10^5 or less. For larger Reynolds number, the motion becomes more erratic, but can still be analyzed in terms of average peak-to-peak variations of Doppler velocity and average oscillation period.

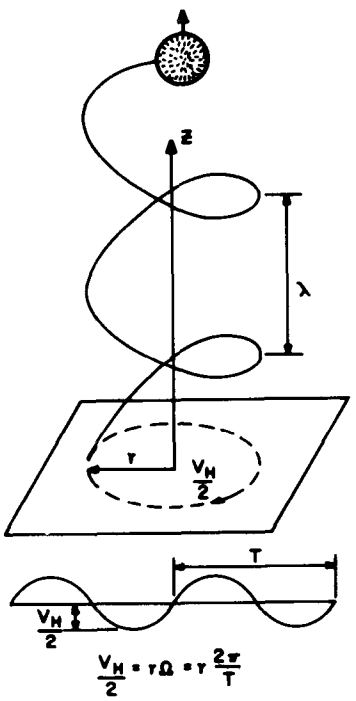

Figure 4. - Helicoidal trajectory parameters, associated with the sinusoidal variation of balloon speed: V_H is the tangential speed, T the period of revolution, and λ the vertical wavelength.

Figures 5 and 6 show examples of the character change of the balloon motion with Reynolds number or balloon diameter. Note in figure 5f the drastic increase of the irregular component of speed owing to an increase of the balloon diameter and ascent rate. For most of the flights, the balloon motion exhibits quasi-regular oscillations, which can be explained on the basis of an helicoidal trajectory specified by the two parameters, r and λ, discussed above.

The Doppler data acquired during 45 flights have been processed according to the above assumptions, with r and λ computed for some of them and presented as a function of balloon size, vertical ascent rate, and Reynolds number. The relationship between λ and R_d is shown in figure 7. One sees that λ increases with R_d from λ = 3 meters when $R_d = 10^4$ to λ = 30 meters when $R_d = 10^6$. The larger values characterize large balloon sizes and fast ascent rates.

The results corresponding to data of Scoggins [1965] (point a) McVehill et al, [1965] (points b, c and d), and Johnson [1965] (point e) are also shown in figure 7. The relationship between wavelength and Reynolds number is approximated by the quadratic expression

$$\lambda = 3.1X10^{-2} (R_d)^{1/2}, \qquad (3)$$

where λ is in meters.

To separate the contribution to R_d from the balloon ascent rate, $\overline{w}$, and the balloon diameter, D, λ has been expressed as a function of D and $\overline{w}$. Figure 8 shows that the relationship between λ and D has a large variance, and figure 9 shows that λ and $\overline{w}$ are correlated even less.

The best parameter to predict λ may be the Reynolds number. Since all measurements were made at about the same altitude, however, the variation of Reynolds number caused by the change of kinematic viscosity has not been explored.

The radius, r, of the circular component of the balloon trajectory has also been computed systematically for all the flights for which periodicity and peak-to-peak variation of the Doppler speed could be determined. The results are in figure 10, where r is plotted versus the balloon diameter, D. The Reynolds number is also in the diagram. For small Reynolds number, r can be approximated by

$$r = D^{3/2}, \qquad (4)$$

where r and D are in meters. For Reynolds number larger than 2 X 10^5, the relationship appears to be different. This may

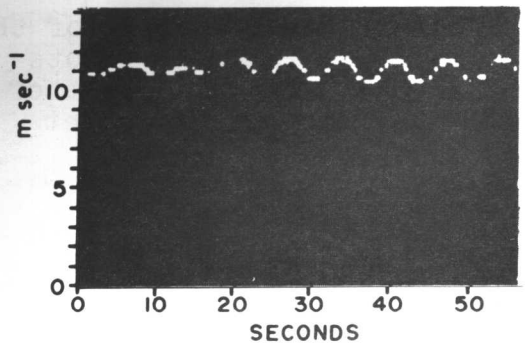

(a). Lift: 38 gm, $\bar{w}$=1m.sec^{-1}, θ=10^{o}
V_H=1.3m.sec^{-1}, T=6.9sec, λ=6.9m.
r=0.71m., r/D=0.77, R_d=4.5X10^4

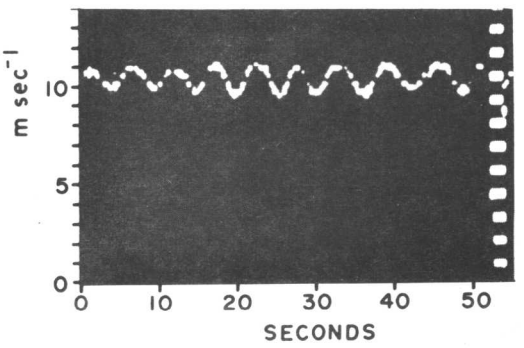

(b). Lift: 74 gm, $\bar{w}$=1.7m.sec^{-1}, θ=11^{o}
V_H=1.65m.sec^{-1}, T=5.7sec, λ=9.6m.
r=0.74m., r/D=0.8, R_d=7X10^4

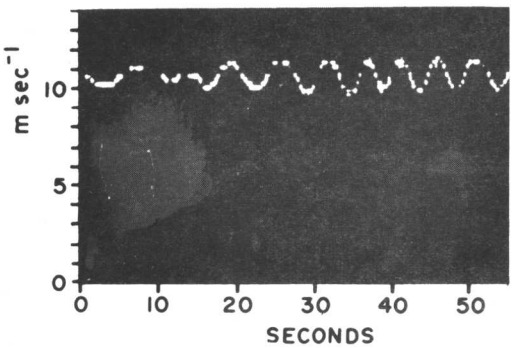

(c). Lift: 85 gm, $\bar{w}$=2.6m.sec^{-1}, θ=15^{o}
V_H=1.9m.sec^{-1}, T=5.2sec, λ=13.5m.
r=0.78m., r/D=0.85, R_d=1.18X10^5

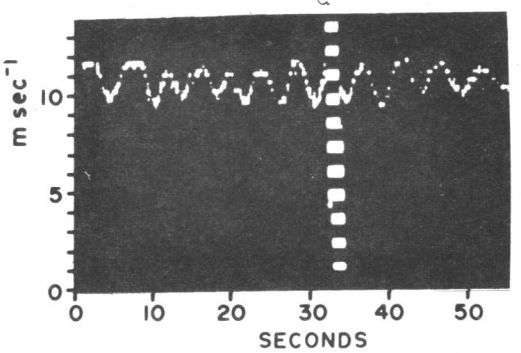

(d). Lift: 167 gm, $\bar{w}$=3.0m.sec^{-1}, θ=20^{o}
V_H=2.4m.sec^{-1}, T=4.4sec, λ=13.2m.
r=0.84m., r/D=0.91, R_d=1.37X10^5

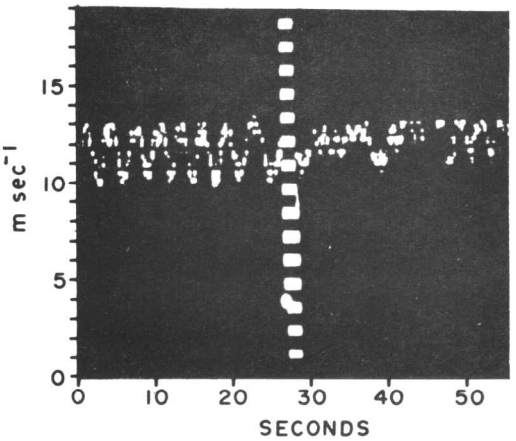

(e). Lift: 260 gm, $\bar{w}$=4.7m.sec^{-1}, θ=27^{o}
V_H=3.3m.sec^{-1}, T=3.1sec, λ=14.7m.
r=0.81m., r/D=0.88, R_d=2.15X10^5

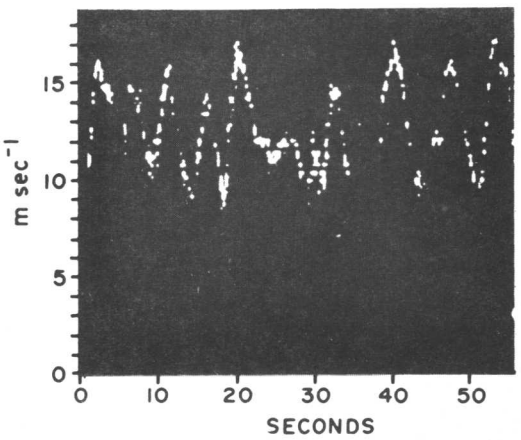

(f). Lift: 670 gm, $\bar{w}$=6.3m.sec^{-1}, θ=35^{o}
V_H=9m.sec^{-1}, T≈6sec, r≈4m.
R_d=4X10^5, (D=48")

Figure 5. - Change of the 100-gm balloon motion with the vertical lift or Reynolds number. Subfigures a, b, c, d, and e, were obtained with the same balloon diameter of 36 inches. Subfigure 5f was obtained with a 48-inch diameter and full lift.

October 12, 1966 Time: 1356 to 1535 CST

30-gm balloons inflated with He + Nitrogen D=24" Mean altitude 1500 m.

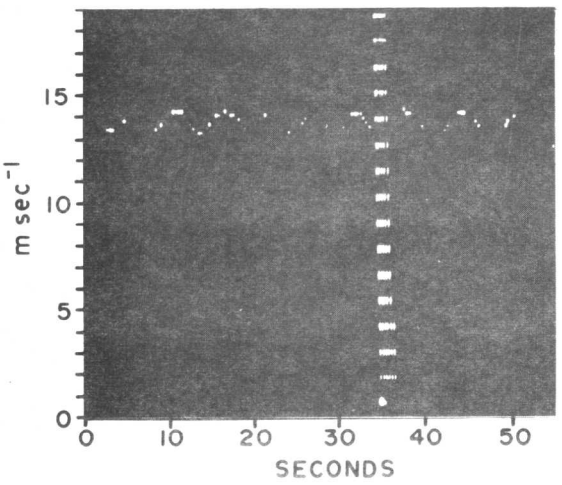

Lift: 7 gm, $\bar{w}$=0.8m.sec^{-1}
V_H=1.2m.sec^{-1}, T=5.5sec, λ=4.4m.
r=0.5m., r/D=0.83, R_d=2.4X10^4

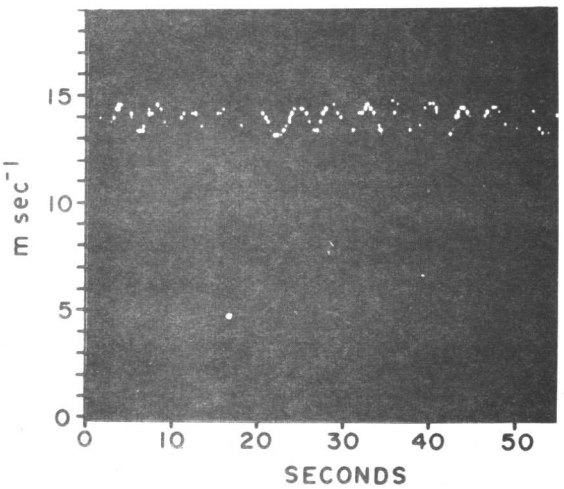

Lift: 20 gm, $\bar{w}$=1.3m.sec^{-1}
V_H=1.5m.sec^{-1}, T=4.0sec, λ=5.2m.
r=0.47m., r/D=0.78, R_d=3.9X10^4

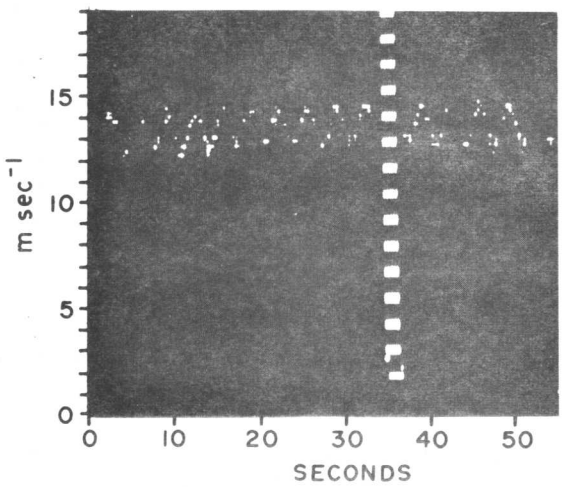

Lift: 32 gm, $\bar{w}$=1.8m.sec^{-1}
V_H=2.5m.sec^{-1}, T=3.2sec, λ=5.7m.
r=0.6m., r/D=1.0, R_d=5.4X10^4

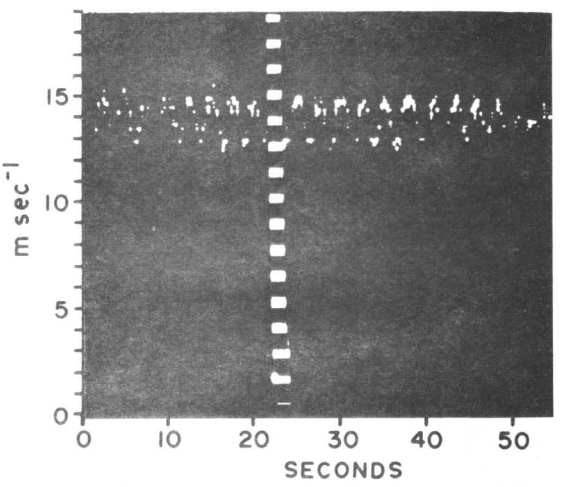

Lift: 57 gm, $\bar{w}$=2.25m.sec^{-1}
V_H=2.8m.sec^{-1}, T=2.6sec, λ=5.85m.
r=0.58m., r/D=0.93, R_d=6.8X10^4

Figure 6. - Time variations of Doppler speed for 30-gm, 24-inch diameter balloons with different vertical ascent rate.

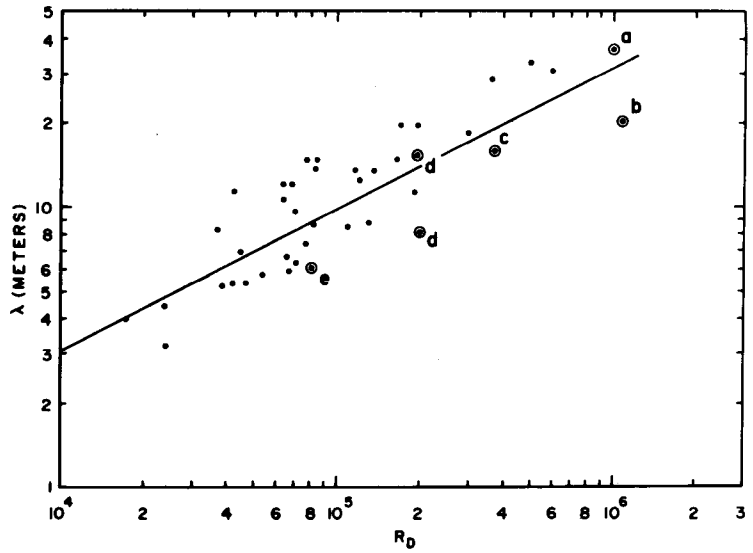

Figure 7. - Relationship between λ and R_d for 42 flights. Circled dots refer to similar data obtained by Scoggins (a), McVehill (b, c and d) and Johnson (e).

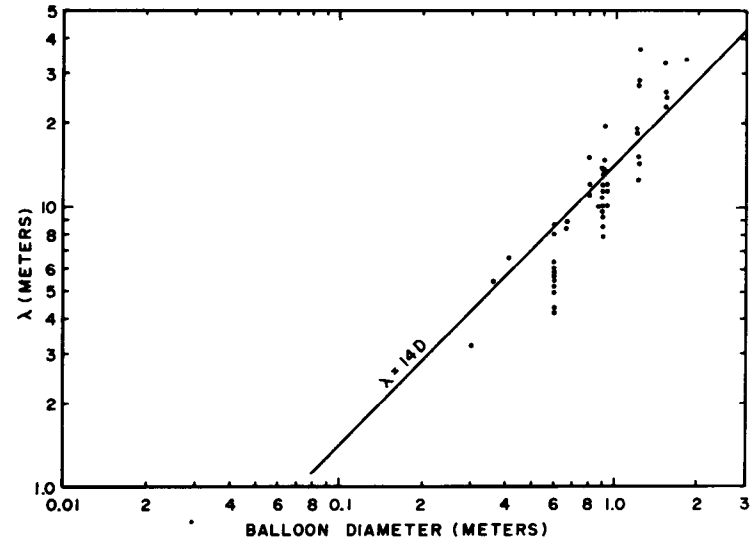

Figure 8. - Relationship between λ and balloon diameter D. The equation λ=14D has been suggested by MacCready [1965].

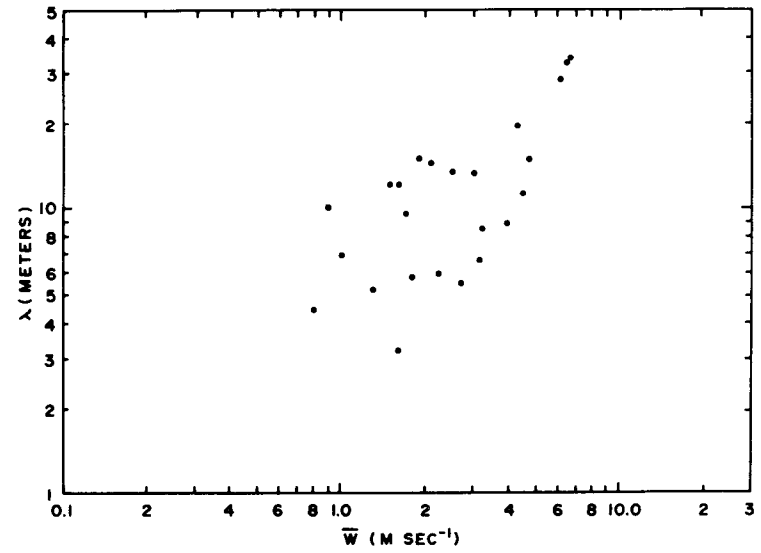

Figure 9. - Relationship between λ and $\overline{w}$ (24 flights).

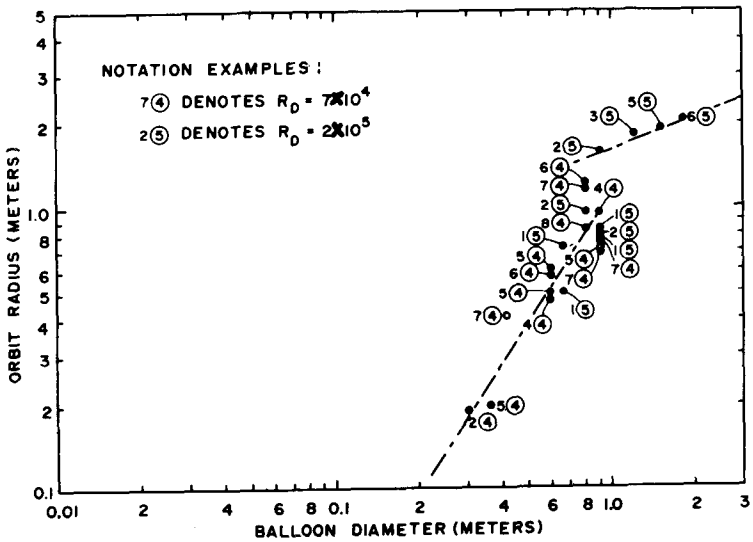

Figure 10. - Relationship between orbit radius and balloon diameter for 26 flights. The Reynolds number is indicated for each flight.

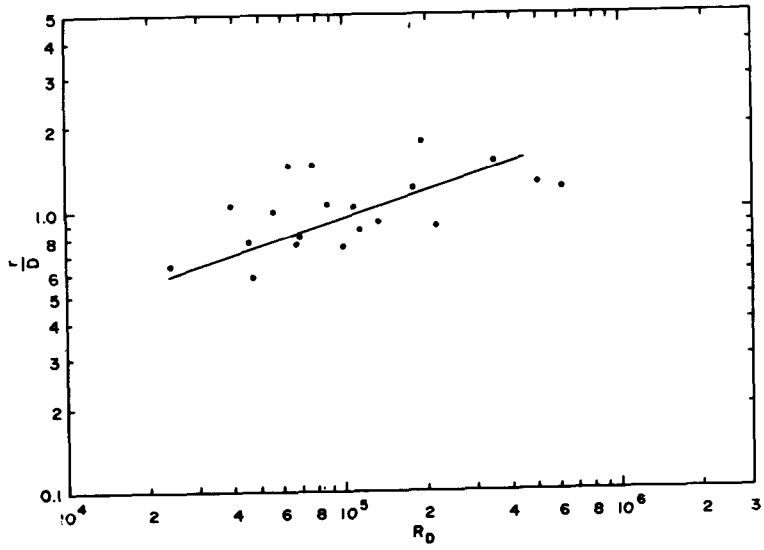

Figure 11. - Relationship of orbit radius, r, to balloon diameter, D, as a function of Reynolds number R_d.

indicate the passage from subcritical regime to supercritical regime which occurs for R_d = 2 X 105 to 3 X 105 in wind tunnel experiments. Figure 11, however, shows that the ratio between r and D is very close to unity, but increases slightly with the Reynolds number.

The ratio r/D can also be expressed as a function of the balloon relative mass, defined by

$$RM = \frac{M_a - L}{Ma} \quad . \qquad (5)$$

Here L is the effective lift force in grams and $M_a = \frac{\pi D^3 \rho_a}{6}$, where D is the sphere diameter in centimeters and ρ_a is the density of the displaced air.

Following MacCready [1965], consider the total amplitude Y_{max} of the regular lateral motion of wavelength λ. In the cases of helicoidal motion, Y_{max} is equal to twice the orbit radius r. MacCready's tests show that

$$Y_{max} = 2r = .2\lambda\ (1 + RM)^{-1}. \qquad (6)$$

With $\lambda = 14D$, also suggested by MacCready, we have

$$\frac{r}{D} = 1.4(1 + 2\ RM)^{-1}. \qquad (7a)$$

In figure 12, r/D is plotted as a function of 1 + 2 RM. Our experimental results indicate that r/D is reasonably explained by the relationship

$$\frac{r}{D} = 2.2(1 + 2RM)^{-1}. \qquad (7b)$$

The relationship (not shown) between r/λ and RM shows much more scattering. This leads to a conclusion that the erratic horizontal displacement of a rising balloon is effectively controlled by the balloon diameter and relative mass. The vertical wavelength λ is not an essential factor.

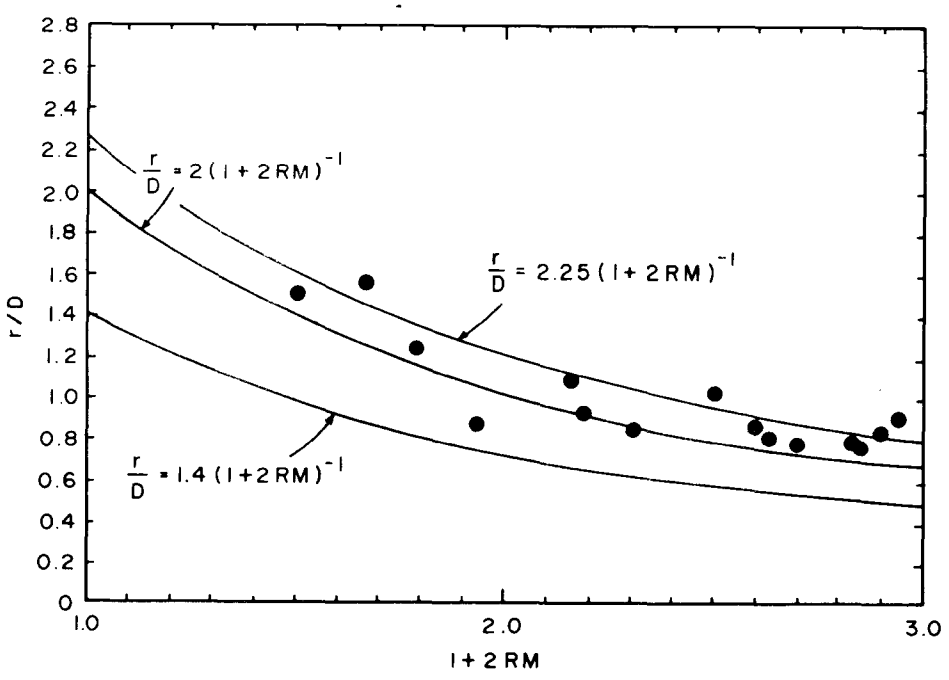

Figure 12. - Relationship between r/D and the balloon relative mass as proposed by MacCready (15 flights).